A nanoscale probe for fluidic and ionic transport

BERTRAND BOURLON[1,2], JOYCE WONG[2], CSILLA MIKÓ[3], LÁSZLÓ FORRÓ[3] AND MARC BOCKRATH[1]*

[1]California Institute of Technology, Mail Stop 128-95, Pasadena, California 91125, USA
[2]Schlumberger-Doll Research, 1 Hampshire Street, Cambridge, Massachusetts 02139, USA
[3]EPFL, CH-1015, Lausanne, Switzerland
*e-mail: mwb@caltech.edu

Published online: 28 January 2007; doi:10.1038/nnano.2006.211

Surface science and molecular biology are often concerned with systems governed by fluid dynamics at the nanoscale, where different physical behaviour is expected[1,2]. With advances in nanofabrication techniques, the study of fluid dynamics around a nano-object or in a nano channel is now more accessible experimentally and has become an active field of research[1,3–5]. However, developing nanoscale probes that can act as flow sensors and that can be easily integrated remains difficult. Many studies demonstrate that carbon nanotubes (CNTs) have outstanding potential for nanoscale sensing, acting as strain[6–8] or charge sensors in chemical[9–11] and biological[12–15] environments. Although nanotube flow sensors composed of bulk nanotubes have been demonstrated[16], they are not readily miniaturized to nanoscale dimensions. Here we report that individual carbon nanotube transistors of ∼2 nm diameter, incorporated into microfluidic channels, locally sense the change in electrostatic potential induced by the flow of an ionic solution. We demonstrate that the nanotube conductance changes in response to the flow rate, functioning as a nanoscale flow sensor.

With diminishing system size, surface-related phenomena become more significant. For example, the ions of an aqueous solution interact electrostatically with charged surfaces, thereby coupling fluid dynamic properties and ionic spatial distribution. This produces electrokinetic phenomena such as electro-osmosis or electrophoresis. In particular, this coupling gives access to the fluid dynamic properties through changes in the electrostatic potential or charge distribution. The small size and high electrical conductivity of CNTs makes them an excellent material for nanoscale electrochemical sensors and probes, a topic that has received much attention in recent times. For example, sensors for the chemical potential of solutions containing redox-active molecules have been demonstrated using single-walled nanotubes[17], and working electrodes have been realized using both single-walled nanotubes (SWNTs)[18] and multiwalled nanotubes (MWNTs)[19].

Although a voltage or current has been observed from fluid flow past bulk nanotubes[16], the change in the conductance of an individual nanotube device in response to fluid dynamic properties has not yet been reported. Here we show that when incorporated into microchannels, electrolytically gated SWNT transistors[20,21] can sense the local potential generated by a fluidic flow of ionic solutions on charged surfaces, known as the streaming potential. From the linear shift of their counterelectrode voltage characteristics versus flow rate Q, we estimate the solution's zeta potential (ζ potential), defined as the electrostatic potential at the no-slip plane of an ionic solution/solid interface. The value of $\zeta \sim -0.1$ V obtained for dilute NaCl solutions contacting a negatively charged silica/PDMS (polydimethylsiloxane) microfluidic channel is similar to previously measured values for indifferent univalent ions Na^+ on silica[22] and K^+ on PDMS (ref. 23).

Furthermore, taking advantage of the coupling between electrostatic potential and fluid dynamics, we demonstrate that individual nanotube transistors act as fluidic flow sensors that locally sense potentials with nanometre-scale resolution. This contrasts with recent studies in which a voltage was generated by flow over bulk quantities of nanotubes[16] or through glass microchannels[24] and measured to determine flow rate. Also, because of their ∼2-nm height, nanotube devices can be integrated into micro- or nanoscale fluidic circuits, making them suitable for use in lab-on-a-chip applications, such as providing active flow sensing and high-resolution flow mapping on surfaces. Another advantage of our approach is that we study the nanotube conductance, using the nanotube transconductance as an amplifier. In particular this ensures that the changes induced by the flow are generated locally from the nanotube only, eliminating potential artefacts that could originate at the electrode level. We estimate for a typical 100 μm × 200 μm microfluidic channel that the thermodynamic limit to sensitivity in a 1 Hz bandwidth is ∼100 nl min^{-1}.

Figure 1a shows a schematic diagram of our experimental geometry where a ∼2 nm diameter single-walled nanotube transistor is integrated inside a microfluidic channel. Details about the device fabrication and measurements are provided in the Methods section. Each nanotube has a source and drain contact through which we applied voltages and measured the resulting current. We also applied a voltage V_{CE} to the counterelectrode, causing ions to migrate to the nanotube surface to form an ionic double layer, which acts as a gate voltage to modulate the charge density within the nanotube. The double layer capacitance is very large at $\sim 4 \times 10^{-9}$ F m^{-1} (refs 20, 21). This gives our devices a very large transconductance $\sim e^2/h$, as first reported by Krüger *et al.*[20] on MWNT devices and later by Rosenblatt *et al.*[21] on SWNT devices. The conductance G of a semiconducting single-walled carbon nanotube versus V_{CE} is shown in Fig. 1b. The data show an insulating region with $G \approx 0$ where the carriers are depleted, and an approximately linear rise in G outside the

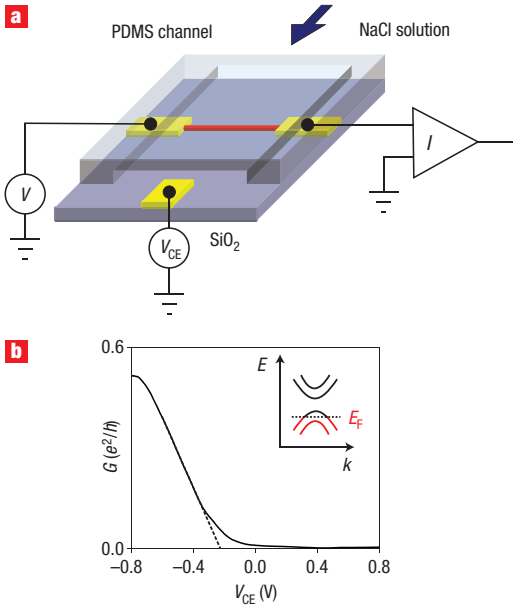

Figure 1 Experimental setup for the nanotube-based flow sensor and nanotube transistor conductance versus counterelectrode voltage. **a**, Schematic diagram of a CNT device showing a nanotube with source, drain and counter electrodes. The device is covered by a PDMS membrane with a microfabricated channel. The channel is placed over the device and liquid is caused to flow through it. **b**, Conductance versus counterelectrode voltage for a semiconducting nanotube device. The inset shows a schematic nanotube band diagram where E_F is the Fermi energy.

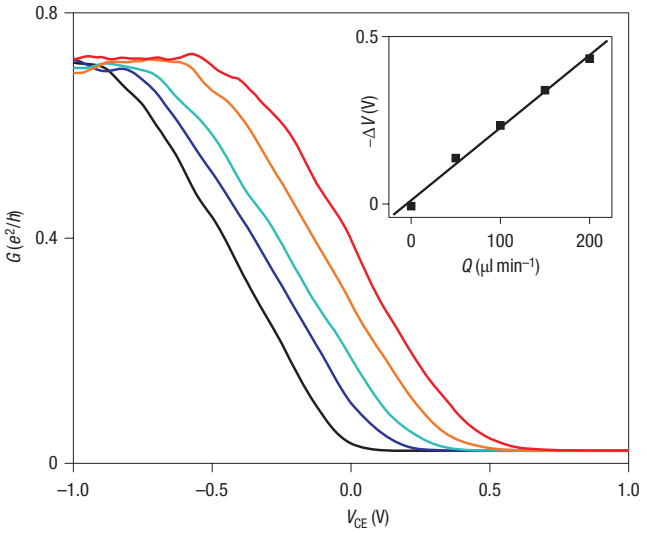

Figure 2 Shift in nanotube transistor threshold voltage with liquid flow rate. Conductance versus counterelectrode voltage for different flow rates (the black, blue, light blue, orange and red curves correspond, respectively, to flow rates of 0, 50, 100, 150 and 200 μl min^{-1}). The inset shows threshold voltage versus flow rate. The data closely follow a linear trend.

insulating region due to hole doping. The inset shows a schematic band diagram of the hole-doped nanotube. We fit a straight line to the curve and extrapolate it to zero conductance to determine the device threshold V_{th}, as shown by the dashed line in Fig. 1b.

When we establish a flow within the channel, V_{th} shifts by an amount ΔV proportional to Q. This is shown in Fig. 2 for equally spaced Q values from 0 to 200 μl min^{-1} for a 0.1 μM NaCl solution. The inset to Fig. 2 shows a plot of ΔV versus Q. The data follow a straight line with a slope $\alpha \approx 2.2$ mV μl^{-1} min. Similar results were also obtained with devices fabricated using MWNTs. Mechanisms coupling fluid flow along the tube axis to electronic transport, such as Coulomb[16] or phonon drag[25], have been proposed previously. However, we found that nanotubes orientated perpendicular to the flow showed similar results, ruling out these possibilities. We therefore consider a model of a nanotube interacting with an ionic solution flowing over a negatively charged surface, as expected for PDMS and SiO_2 in contact with an aqueous solution[23,26]. The charged surface attracts positively charged ions, forming an ionic double layer. The fluid flow drives the ions in the double layer along the surface while a counterbalancing electric field maintains the steady-state condition of zero net charge current, generating the electrochemical streaming potential.

Approximating the channel geometry to be cylindrical, the electrostatic potential drop in the channel is given by

$$\Delta V = \varepsilon\varepsilon_0 QR\zeta/[\eta e(n+\lambda)\mu] \qquad (1)$$

where ε is the fluid dielectric constant, ε_0 is the vacuum permittivity, R is the flow resistance from the tube to the counterelectrode, estimated from Poiseuille's law, ζ is the zeta potential of the ionic double layer on the channel surfaces, η is the liquid viscosity, n is the ionic concentration, λ is an offset concentration that may arise from the background concentration of ions and/or surface conductivity along the channel walls, and μ is the effective ionic mobility[26]. The effective counterelectrode voltage that induces the charge on the nanotube is given by $\phi = V_{CE} - \Delta V$, which produces a shift of ΔV in V_{th}. From equation (1), we expect that for sufficiently large n, ΔV should decrease as n^{-1}.

Figure 3 shows a plot of the slope α of the threshold voltage shift versus Q for a number of values of n, with NaCl as the electrolyte. The inset to Fig. 3 shows G versus V_{CE} for several n values, from which the data were determined. Fitting our data to the above relation for $\alpha = |\mathrm{d}(\Delta V)/\mathrm{d}Q|$ with $\varepsilon\varepsilon_0 = 8 \times 10^{-10}$ F m^{-1}, $R = 7 \times 10^{10}$ Pa s m^{-3}, $\eta = 0.9 \times 10^{-3}$ Pa s and $\mu \sim 10^{-7}$ m^2 V^{-1} s^{-1}, yields $\lambda \sim 10^{-6}$ M and $\zeta \sim -0.1$ V. As the ζ potential depends weakly on concentration for the dilute ionic concentrations used here[22,26], the value we have obtained is only an estimate. Nevertheless, our value for the ζ potential is in good agreement with typical values previously reported for several dilute ionic solutions in contact with glass and PDMS-coated channels[22,23]. The value for λ can be accounted for by the ionic concentration due to the measured pH of our deionized water, which is typically in the range 5–6, and therefore we assume that the surface conductivity contribution to λ is of a similar order of magnitude or smaller.

The ability of nanotubes to sense the local streaming potential enables our devices to act as integrated nanoscale flow sensors. Figure 4 shows a plot of G versus time at constant V_{CE} as the flow rate is increased sequentially through 0, 100, 200 and 300 μl min^{-1}, and then back down sequentially through the same values. This produces a series of steps in the device conductance. Note that the oscillations in the conductance on the steps are due to periodic variations in Q produced by the axial motion of the syringe pump. V_{CE} can be set where G versus V_{CE} is linear so that the change in G on each step is directly proportional to its corresponding Q, as expected from equation (1) (Fig. 4 inset).

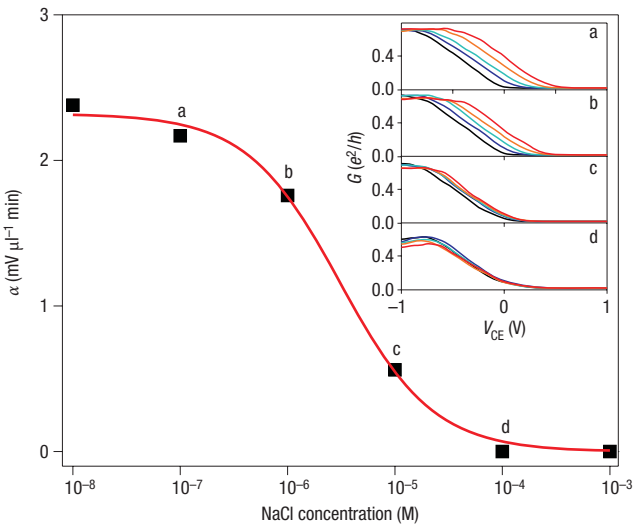

Figure 3 Nanotube transistor threshold shift for different ionic concentrations. Parameter α (slope of threshold voltage versus flow rate) versus NaCl concentration. The inset shows conductance versus counterelectrode voltage data, where a–d indicate concentrations according to the points a–d in the main panel from which α was extracted.

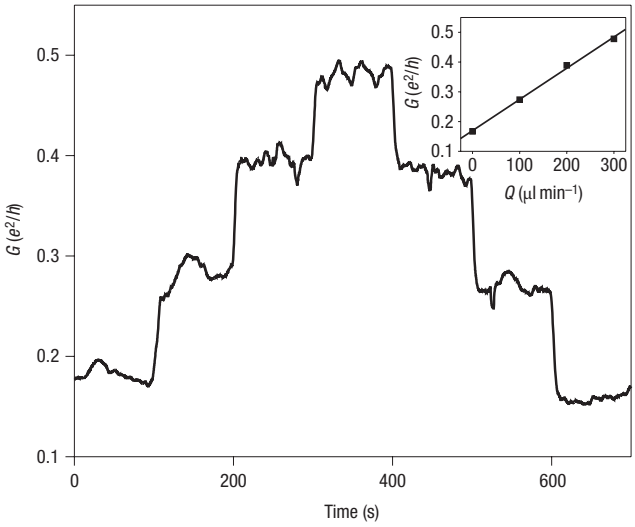

Figure 4 Flow sensor operation. Conductance versus time for a semiconducting nanotube device as the flow rate is stepped up sequentially through 0, 100, 200 and 300 μl min^{-1}, and then back down sequentially through the same values. V_{CE} is held constant at −0.2 V. The inset shows nanotube conductance versus flow rate, in which the device acts as a flow sensor.

To estimate the fundamental limits to flow sensing using our technique, we assume that Johnson noise from the fluid resistance is the ultimate limit to the sensitivity. Johnson noise introduces thermal fluctuations δV_{CE} to the voltage applied to the electrolytic gate. We estimate $\delta V_{CE} \sim 100\ \mu V\ Hz^{-1/2}$ for $n = 10^{-6}$ M. Based on the measured values of α, the lowest detectible flow rate in our channel in a 1 Hz bandwidth would be $Q \sim 100$ nl min^{-1}. In our experiments, we have detected flow rates as small as ~25 μl min^{-1} with MWNT devices and somewhat larger for SWNT devices. This is 2–3 orders of magnitude larger than the fundamental limit imposed by thermodynamics. Although much of the observed lower limit is likely due to the syringe pump and its known stability limits, considerable improvements in intrinsic device sensitivity may be made, for example, by using longer nanotubes to reduce the intrinsic device noise[27].

In conclusion, we have demonstrated that individual CNT transistors can be used to probe electrokinetic phenomena and fluid flow in microfluidic channels. We note that, in addition to the changes of transistor threshold voltage observed here, a careful analysis of changes in transconductance can be very interesting. Indeed, the nanotube transconductance reflects the organization of ions in the double layer around the nanotube. In particular, this double layer should be directly perturbed by the flow in the case of nanoscale channels or when working with suspended nanotubes. Such miniaturization of fluidic channels to the nanoscale has already been demonstrated[1,3–5]. Following what has been demonstrated here in microscale channels, the incorporation of these electrolytic transistors in nanoscale channels should yield a novel approach for investigating electrokinetic phenomena and fluid dynamics at the nanometre scale, where new behaviour may emerge.

METHODS

The ~2-nm diameter SWNT transistors used in this experiment were fabricated by nanotube growth from catalytic islands[28], followed by electron-beam lithography, metal evaporation and liftoff. MWNTs (provided by L. Forró's group) were also used in this study, but only data from SWNTs are included in this report. Semiconducting nanowires could also be considered for this experiment. However, nanotubes are particularly well suited for the task because of their atomic regularity, chemical inertness and lack of surface oxidation. Cr/Au source and drain contacts were used for the MWNTs and Pd/Au (ref. 29) source and drain contacts for the SWNTs. The completed devices were covered by a PDMS membrane (without oxygen plasma cleaning), in which a 100-μm-high, 200-μm-wide and 5-mm-long fluidic channel was defined by replication moulding using SU-8/silicon masters made by optical lithography[30]. A syringe was filled with a NaCl solution and attached to the inlet though a capillary. The syringe was then driven by a syringe pump to inject fluid at a well-controlled rate into the channel. We positioned the channel such that fluid injected into it flowed directly over the nanotube devices. The entire chip was held at an angle and the drop of liquid that collected outside the outlet was allowed to contact a gold bonding pad, which was used as a counterelectrode. Data to study the voltage shift were collected using a lock-in amplifier with a bias voltage of 0.1 V and a frequency of a few kHz. We note that voltage shifts have been observed in more than ten devices in response to flow rate. From eight of them it was possible to estimate the parameter α (slope of voltage shift versus flow rate) at low ionic concentration ($n \leq 10^{-6}$ M). The values of α were found to range between 1.5 and 4.5 mV μl^{-1} min.

Received 9 October 2006; accepted 21 December 2006; published 28 January 2007.

References

1. Eijkel, J. C. T. & van den Berg, A. Nanofluidics: what is it and what can we expect from it? *Microfluid. Nanofluid.* **1,** 249–267 (2005).
2. Israelachvilli, J. N., McGuiggan, P. M. & Homola, A. M. Dynamic properties of molecularly thin liquid films. *Science* **240,** 189–191 (1988).
3. van der Heyden, F. H. J., Stein, D. & Dekker, C. Streaming currents in a single nanofluidic channel. *Phys. Rev. Lett.* **95,** 116104 (2005).
4. Li, J. *et al.* Ion-beam sculpting at nanometre length scales. *Nature* **412,** 166–169 (2001).
5. Han, J. & Craighead, H. G. Separation of long DNA molecules in a microfabricated entropic trap array. *Science* **288,** 1026–1029 (2000).
6. Cao, J., Wang, Q. & Dai, H. J. Electromechanical properties of metallic, quasimetallic, and semiconducting carbon nanotubes under stretching. *Phys. Rev. Lett.* **90,** 157601 (2003).
7. Minot, E. D. *et al.* Tuning carbon nanotube band gaps with strain. *Phys. Rev. Lett.* **90,** 156401 (2003).
8. Yang, L. & Han, J. Electronic structure of deformed carbon nanotubes. *Phys. Rev. Lett.* **85,** 154–157 (2000).
9. Kong, J. *et al.* Nanotube molecular wires as chemical sensors. *Science* **287,** 622–625 (2000).

10. Staii, C., Johnson, A. T., Chen, M. & Gelperin, A. DNA-decorated carbon nanotubes for chemical sensing. *Nano Lett.* **5,** 1774–1778 (2005).
11. Bradley, K., Gabriel, J. C. P., Briman, M., Star, A. & Gruner, G. Charge transfer from ammonia physisorbed on nanotubes. *Phys. Rev. Lett.* **91,** 218301 (2003).
12. Bradley, K., Briman, M., Star, A. & Gruner, G. Charge transfer from adsorbed proteins. *Nano Lett.* **4,** 253–256 (2004).
13. Boussaad, S., Tao, N. J., Zhang, R., Hopson, T. & Nagahara, L. A. In situ detection of cytochrome c adsorption with single walled carbon nanotube device. *Chem. Commun.* **13,** 1502–1503 (2003).
14. Besteman, K., Lee, J. O., Wiertz, F. G. M., Heering, H. A. & Dekker, C. Enzyme-coated carbon nanotubes as single-molecule biosensors. *Nano Lett.* **3,** 727–730 (2003).
15. Gao, M., Dai, L. & Wallace, G. G. Glucose sensors based on glucose-oxidase-containing polypyrrole/aligned carbon nanotube coaxial nanowire electrodes. *Synthetic Met.* **137,** 1393–1394 (2003).
16. Ghosh, S., Sood, A. K. & Kumar, N. Carbon nanotube flow sensors. *Science* **299,** 1042–1044 (2003).
17. Larrimore, L., Nad, S., Zhou, X., Abruna, H. & McEuen, P. L. Probing electrostatic potentials in solution with carbon nanotube transistors. *Nano Lett.* **6,** 1329–1333 (2006).
18. Heller, I. *et al.* Individual single-walled carbon nanotubes as nanoelectrodes for electrochemistry. *Nano Lett.* **5,** 137–142 (2005).
19. Campbell, J. K., Sun, L. & Crooks, R. M. Electrochemistry using single carbon nanotubes. *J. Am. Chem. Soc.* **121,** 3779–3780 (1999).
20. Kruger, M., Buitelaar, M. R., Nussbaumer, T., Schonenberger, C. & Forro, L. Electrochemical carbon nanotube field-effect transistor. *Appl. Phys. Lett.* **78,** 1291–1293 (2001).
21. Rosenblatt, S. *et al.* High performance electrolyte gated carbon nanotube transistors. *Nano Lett.* **2,** 869–872 (2002).
22. Kirby, B. J. & Hasselbrink, E. F. Zeta potential of microfluidic substrates: 1. Theory, experimental techniques, and effects on separations. *Electrophoresis* **25,** 187–202 (2004).
23. Sze, A., Erickson, D., Ren, L. & Li, D. Zeta-potential measurement using the Smoluchowski equation and the slope of the current–time relationshp in electroosmotic flow. *J. Colloid Interface Sci.* **261,** 402–410 (2003).
24. Kim, D.-K., Majumdar, A. & Kim, S. J. Electrokinetic flow meter. *Sensor Actuat. A-Phys.* (2006).
25. Kral, P. & Shapiro, M. Nanotube electron drag in flowing liquids. *Phys. Rev. Lett.* **86,** 131–134 (2001).
26. Hunter, R. J. *Foundations of Colloid Science* (Oxford Univ. Press, New York, 2001).
27. Ishigami, M. *et al.* Hooge's constant for carbon nanotube field effect transistors. *Appl. Phys. Lett.* **88,** 203116 (2006).
28. Kong, J., Soh, H.T., Cassell, A.M., Quate, C.F. & Dai, H. Synthesis of individual single-walled carbon nanotubes on patterned silicon wafers. *Nature* **395,** 878–881 (1998).
29. Mann, D., Javey, A., Kong, J., Wang, Q. & Dai, H. J. Ballistic transport in metallic nanotubes with reliable Pd ohmic contacts. *Nano Lett.* **3,** 1541–1544 (2003).
30. Duffy, D. C., McDonald, J. C., Schueller, O. J. A. & Whitesides, G. M. Rapid prototyping of microfluidic system poly(dimethylsiloxane). *Anal. Chem.* **70,** 4974–4984 (1998).

Acknowledgements

The authors wish to thank the Micro/Nano Fabrication Laboratory at Caltech where the sample fabrication was performed. This work was sponsored by Schlumberger. The work in Lausanne was supported by the Swiss NSF and its NCCR 'Nanoscale Science'.

Author contributions

B.B., J.W. and M.B. conceived and designed the experiments. B.B. and J.W. performed the experiments. B.B., J.W. and M.B. analysed the data. C.M. and L.F. contributed materials (multiwalled nanotubes). B.B., J.W. and M.B. co-wrote the paper. All authors discussed the results and commented on the manuscript.

Competing financial interests

The authors declare that they have no competing financial interests.